Europace (2015) **17**, 483–488
doi:10.1093/europace/euu263



# Wideband late gadolinium enhanced magnetic resonance imaging for imaging myocardial scar without image artefacts induced by implantable cardioverter-defibrillator: a feasibility study at 3 T

**Ravi Ranjan[1]*, Christopher J. McGann[1], Eun-Kee Jeong[2], KyungPyo Hong[2], Eugene G. Kholmovski[1,2], Josh Blauer[1], Brent D. Wilson[1], Nassir F. Marrouche[1], and Daniel Kim[2]**

[1]CARMA Center, Division of Cardiology, Internal Medicine, University of Utah, 30 North 1900 East, Rm 4A100, Salt Lake City, UT 84132, USA; and [2]UCAIR, Department of Radiology, University of Utah, Salt Lake City, UT, USA

*Received 21 May 2014; accepted after revision 26 August 2014; online publish-ahead-of-print 21 October 2014*

**Aim** Late gadolinium enhanced (LGE) magnetic resonance imaging (MRI) is a useful tool for facilitating ventricular tachycardia (VT) ablation. Unfortunately, most VT ablation candidates often have prophylactic implantable cardioverter-defibrillator (ICD) and do not undergo cardiac MRI largely due to image artefacts generated by ICD. A prior study has reported success of 'wideband' LGE MRI for imaging myocardial scar without image artefacts induced by ICD at 1.5T. The purpose of this study was to widen the availability of wideband LGE MRI to 3T, since it has the potential to achieve higher spatial resolution than 1.5T.

**Methods and results** We compared the performance of standard and wideband LGE MRI pulse sequences in phantoms and canines with myocardial lesions created by radiofrequency ablation. Standard LGE MRI produced image artefacts induced by ICD and 49% accuracy in detecting 97 myocardial scars examined in this study, whereas wideband LGE MRI produced artefact-free images and 94% accuracy in detecting scars. The mean image quality score (1 = nondiagnostic, 2 = poor, 3 = adequate, 4 = good, 5 = excellent) was significantly ($P < 0.001$) higher for wideband ($3.7 \pm 0.8$) than for standard LGE MRI ($2.1 \pm 0.7$). The mean artefact level score (1 = minimal, 2 = mild, 3 = moderate, 4 = severe, 5 = nondiagnostic) was significantly ($P < 0.001$) lower for wideband ($2.1 \pm 0.8$) than for standard LGE MRI ($4.0 \pm 0.6$). Wideband LGE MRI agreed better with gross pathology than standard LGE MRI.

**Conclusion** This study demonstrates the feasibility of wideband LGE MRI for suppression of image artefacts induced by ICD at 3T.

**Keywords** Ventricular tachycardia • Radiofrequency ablation • Late gadolinium enhanced magnetic resonance imaging • Implantable cardioverter-defibrillator

## Introduction

Radiofrequency (RF) ablation is clinically indicated for treating ventricular tachycardia (VT),[1] where the clinical goal is to identify and ablate border zones of scar areas which are known to be substrates for arrhythmia[2] and maintaining VT.[3] However, it is very challenging to identify these substrates during VT using standard electro-anatomical voltage mapping due to haemodynamic instability in arrhythmia.[4] To circumvent this problem, scar areas and border zones are typically identified using electro-anatomical voltage mapping in sinus rhythm and previously defined amplitude thresholds[5] to target VT ablation sites. Given these limitations, VT ablation guided by electro-anatomical voltage mapping in sinus rhythm frequently misses border zones, especially if the target is mid-myocardial or epicardial. Consequently, not ablating these substrates could lead to future VT events.[6,7]

Late gadolinium enhanced (LGE)[8] magnetic resonance imaging (MRI) is the most proven test for detection of scar, and it has been

* Corresponding author. Tel: +1 801 213 2273; fax: +1 801 581 7735. *E-mail address*: ravi.ranjan@hsc.uah.edu

## What's new

- Wideband late gadolinium enhanced (LGE) magnetic resonance imaging (MRI) enables suppression of image artefact induced by implantable cardioverter-defibrillator (ICD) at 3 T
- Wideband LGE MRI with ICD agrees with gross pathology of post-mortem tissue and 3D LGE MRI without ICD
- Scar map derived from artefact-free wideband LGE images shows the exact distribution of scar in the left ventricle

used to facilitate VT ablation.[9,10] Magnetic resonance imaging of VT ablation candidates is technically challenging, because they often have prophylactic implantable cardioverter-defibrillator (ICD). Despite the fact that MRI can be performed safely in most patients with non-MR compatible ICDs at 1.5T,[11,12] many patients who would derive benefit from MRI do not undergo MRI largely due to image artefacts arising from ICD. Specifically, an ICD located 5–10 cm away from the heart can induce a centre frequency shift as large as 2–6 kHz,[13] which renders a standard inversion RF pulse used in LGE MRI to be ineffective and generate hyper-intense image artefacts.

Recently, the feasibility of wideband LGE MRI was demonstrated for assessment of myocardial scarring in patients with non-MR compatible ICD at 1.5T.[13] Widening the availability wideband of LGE MRI to all clinical scanners, including 3 T, is important since approximately one-third of clinical MR scanners in the USA are 3 T, and since 3 T enables higher spatial resolution for better detection of border zones.[14] Currently, two major cardiac device manufacturers have produced Food and Drug Administration-approved, MR-compatible pacemakers for the US market, and one of them is conducting a clinical trial for MR-compatible ICDs. These new cardiac device developments are likely to lead to new studies aimed at establishing procedures for safe MRI of patients with ICD at 3 T. The purpose of this study was to demonstrate the feasibility of wideband LGE MRI for suppression of image artefacts induced by ICD at 3T.

# Methods

## Magnetic resonance imaging hardware

A wideband LGE MRI pulse sequence (see below) was implemented on a 3 T whole-body MRI scanner (Verio, Siemens Healthcare, Erlangen, Germany), equipped with a gradient system capable of achieving a maximum gradient strength of 45 mT/m and a slew rate of 200 T/m/s. The RF excitation was performed using the body coil, and a 32-element cardiac coil (RAPID MR International) was used for signal reception.

## Pulse sequence

We implemented a wideband LGE MRI pulse sequence by using a commercially available adiabatic hyperbolic secant pulse (Siemens VB17 platform) set with the following parameters: frequency modulation parameter $\beta = 750$ radians/s, phase modulation parameter $\mu = 10$ (dimensionless), and pulse duration 6.1 ms. We performed a preliminary phantom experiment to calibrate the frequency bandwidth and observed that the bandwidth was 1 and 4 kHz for standard [i.e. Siemens VB17 platform, $\beta = 672$ radians/s, $\mu = 5$ (dimensionless), and pulse duration = 10.2 ms] and wideband inversion RF pulses, respectively (see Supplementary material online, *Figure S1*). To achieve the adiabatic condition within the hardware limit of the RF amplifier, wideband hyperbolic secant inversion RF pulse was set to achieve nominal RF field ($B_1+$) of 779 Hz over the pulse duration of 6.1 ms. For reference, standard hyperbolic secant inversion pulse is set to achieve nominal $B_1+$ of 750 Hz over the pulse duration of 10.2 ms. We note that the wideband inversion pulse was specifically designed to deposit lower RF energy than the standard inversion pulse, thereby guaranteeing that wideband LGE MRI will produce lower global-specific absorption rate (SAR) than standard LGE MRI at 3 T.

## Initial evaluation in a phantom with implantable cardioverter-defibrillator and intracardiac leads

We evaluated the performance of standard and wideband LGE MRI pulse sequences with inversion time (TI) = 210 ms to null the signal of a phantom ($T_1 = 303$ ms) with an ICD generator (Lumax 540 DR-T, BIOTRONIK) taped to one side of the phantom as shown in *Figure 1*. We performed LGE MRI in a coronal plane with ICD in the plane, to visualize the effectiveness of inversion pulses as a function of ICD distance. For reference, a proton density image was also acquired (i.e. without the inversion pulse). The same experiment was repeated with intracardiac leads attached to the same location. Imaging parameters were kept identical to those used for animal MRI (see Animal magnetic resonance imaging experiment).

## Animal model with ventricular scar

Seven canines (weighting 29–35 kg) were imaged to evaluate the effectiveness of wideband LGE MRI. Radiofrequency ablation was performed to create discrete scars in the right ventricle (RV) and left ventricle (LV). In the electrophysiology suite, canines were anaesthetized using propofol and then intubated to maintain them in a surgical plane of anaesthesia with 1.5–3% isoflurane with a ventilator (DRE Premier XP MRI-Compatible Veterinary Anesthesia Machine, DRE Veterinary). Right and left femoral vein access was obtained using percutaneous puncture. A 11 Fr sheath (St. Jude Medical) was inserted into the left femoral vein and was used to insert an intracardiac echocardiogram (ICE) probe. A 8.5 Fr sheath was inserted into the right femoral vein. Under fluoroscopic and ICE guidance, transeptal puncture was made to access the left atrium. Through the 8.5 Fr sheath, an ablation catheter (Thermocool, Biosense Webster) was advanced to the LV cavity. Radio frequency ablation was carried out using 25–50 W for 30 s at multiple discrete spots of the ventricles, and ablated areas were marked on the electro-anatomical map (CARTO, Biosense Webster). The study protocol was approved by the Institutional Animal Care and Use Committee at the University of Utah.

## Animal magnetic resonance imaging experiment

After RF ablation, animals were transported to the MR scanner for imaging. Throughout the MRI experiments, animals were ventilated and maintained in a surgical plane of anaesthesia as described above. Magnetic resonance imaging experiments were conducted with the dogs in lateral recumbency. Anterior and posterior RF receiver coils were positioned to cover the heart.

The ICD generator was taped on the left shoulder, ~10 cm away from the heart. Gadolinium enhanced MRI was performed ~15–20 min after administration of contrast agent (0.15 mmol/kg of MultiHance, Bracco Diagnostics, Inc.), using both standard and wideband LGE pulse sequences. Single-shot LGE MRI was performed to cover the entire heart in short-axis planes (~12–14 slices) during breath-hold

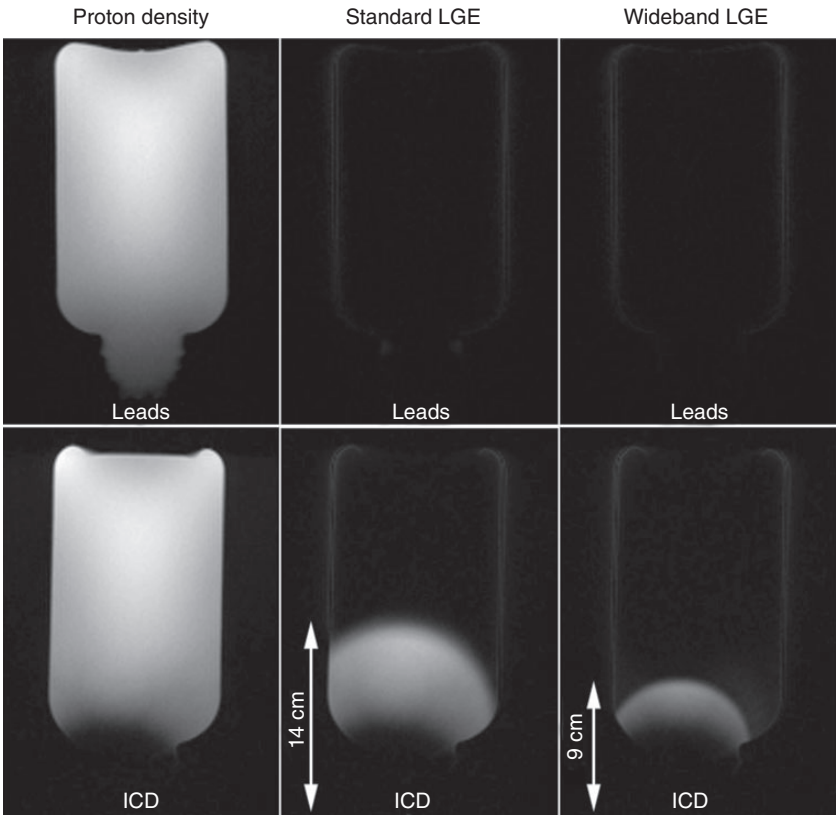


**Figure 1** Coronal LGE images of a phantom with ICD taped on one side of the phantom as shown (bottom row). As a reference, a proton density image (left) was acquired without the inversion pulse. Standard and wideband LGE MRI was performed with TI = 210 ms to null the signal of the phantom (with known $T_1$ = 303 ms). Standard (middle) and wideband (right) IR pulses. Bright regions in LGE images correspond to image artefact. The corresponding images with intracardiac leads taped on the same location (top row). Images are displayed with identical grayscales (0–1000 a.u.).

via the respirator. Imaging parameters were identical between the two pulse sequences (except for the inversion pulse) which included: field of view = 280 mm × 180 mm (phase-encoding), matrix = 192 × 123, in-plane resolution = 1.5 × 1.5 mm, slice thickness = 7 mm, generalized autocalibrating partially parallel acquisitions[15] acceleration factor = 1.8, receiver bandwidth = 744 Hz/pixel, flip angle = 20°, echo time = 1.7 ms, LGE MRI applied every two or three cardiac cycles (depending on heart rate), TI = 280–400 ms. A TI scout pulse sequence[16] was used to identify the TI to null the normal myocardium. While this TI scout pulse sequence generated considerable image artefacts induced by ICD, it was adequate to identify the TI to null the normal myocardium. The pulse sequence order (standard vs. wideband) was randomized to minimize potential bias.

To further validate our 2D LGE results, we performed 3D LGE MRI[17] without the ICD, and reformatted the 3D LGE image set to match the corresponding 2D planes. The reformatted images were then used as references to visually match the RF lesions by two expert readers in consensus. Using 3D LGE MRI as the reference, we calculated the accuracy in detecting LV RF lesions with standard and wideband LGE MRI. The relevant imaging parameters of 3D LGE MRI include spatial resolution = 1.5 × 1.5 × 2.5 mm and scan time ~ 5 min with navigator gating.

## Animal euthanasia, gross pathology

After the MRI, animals were euthanized while under general anaesthesia, with KCl (200 mg/kg, IV) for heart removal and evaluation. Immediately before euthanasia, 120 mL of 20% 2, 3, 5-triphenyltetrazolium chloride in 0.9% NaCl solution was administered via IV, as a vital stain to distinguish between viable and non-viable myocardium. Excised hearts were fixed in 10% buffered formalin and then sectioned in short-axis planes of 2.5 mm thickness to match the LGE MR images.

## Three-dimensional scar maps

A stack of short-axis wideband LGE images covering the whole LV was used to map the scar areas in 3D. Endocardial contours of the LV (red) and RV (purple) were defined using an edge preserving, smoothing filter followed by user-defined thresholding in the Seg3D software (University of Utah). Identification of ablated tissues and the LV wall, as well as removal of venous structures and other chambers, was performed by manual segmentation. Three dimensional surface meshes were constructed and rendered in the SCIRun 4.6 software (University of Utah).

## Image quality evaluation

A total of 74 (37 standard and 37 wideband) LGE images with different RF lesions per imaging plane were pooled and randomized for blinded qualitative evaluation. Two readers (C.J.M., Level 3 with 12 years of experience; B.D.W., Level 3 with 8 years of experience) independently evaluated the image quality and artefact using a five-point Likert scale: image quality for conspicuity of RF lesion (1 = nondiagnostic, 2 = poor, 3 = adequate, 4 = good, 5 = excellent) and overall artefact level (1 = minimal, 2 = mild, 3 = moderate, 4 = severe, 5 = nondiagnostic),

including those that are unrelated to ICD. The two readers were blinded to each other and image type.

### Statistical analysis

The reported image quality and artefact scores, which were initially averaged over two readers, represent the mean ± standard deviation over 37 LGE images. For each category, the Wilcoxon rank-sum test was used to compare the two scores, where $P < 0.05$ was considered to be statistically significant. In addition, we calculated the inter-reader agreement in image quality and artefact scores using the Bland–Altman analysis. Statistical analysis was performed using the Analyse-it software (Analyse-it Software, Leeds, United Kingdom).

## Results

### Phantom study

*Figure 1* shows coronal LGE images of a phantom with ICD taped on one side of the phantom as shown. A proton density image (i.e. without the inversion pulse) is also shown as a reference. Standard LGE MRI yielded considerable image artefacts, whereas wideband LGE MRI suppressed image artefacts in regions that are greater than 10 cm away from the ICD. *Figure 1* also shows the corresponding images with intracardiac leads attached to the same location as ICD. Note that both standard and wideband LGE were unaffected by intracardiac leads.

### Animal study

*Figure 2* representative LGE images of three different dogs with RF lesions, acquired using standard and wideband inversion pulses. Compared with standard LGE MRI, wideband LGE MRI yielded no significant image artefacts. Moreover, wideband LGE MRI agreed better with gross pathology than standard LGE MRI. The corresponding 3D scar map derived from wideband LGE images (same animal shown in *Figure 2*, top row) is shown in *Figure 3*, where all scars were visible. A similar 3D scar map was not generated from standard LGE images due to considerable image artefacts.

In all seven animals (37 standard and 37 wideband LGE images total), standard LGE MRI yielded large artefacts while wideband LGE MRI exhibited no significant artefacts and enabled complete identification of RF ablation lesions. The mean image quality score was significantly ($P < 0.001$) higher for wideband ($3.7 \pm 0.8$) than standard LGE MRI ($2.1 \pm 0.7$). The mean artefact level was significantly ($P < 0.001$) lower for wideband ($2.1 \pm 0.8$) than standard LGE MRI ($4.0 \pm 0.6$). According to the Bland–Altman analysis, for image quality scores, the mean difference was 0.01 and the upper and lower 95% limits of agreement were 1.2 and −1.1, respectively. For image artefact scores, the mean difference was 0.4, and the upper and lower 95% limits of agreement were 1.6 and −1.4, respectively.

Compared with 3D LGE without ICD (97 LV RF lesions in total), wideband LGE with ICD yielded 93.8% accuracy in detecting RF lesions by expert readers in consensus, whereas standard LGE with ICD yielded 48.5% accuracy in detecting RF lesions.

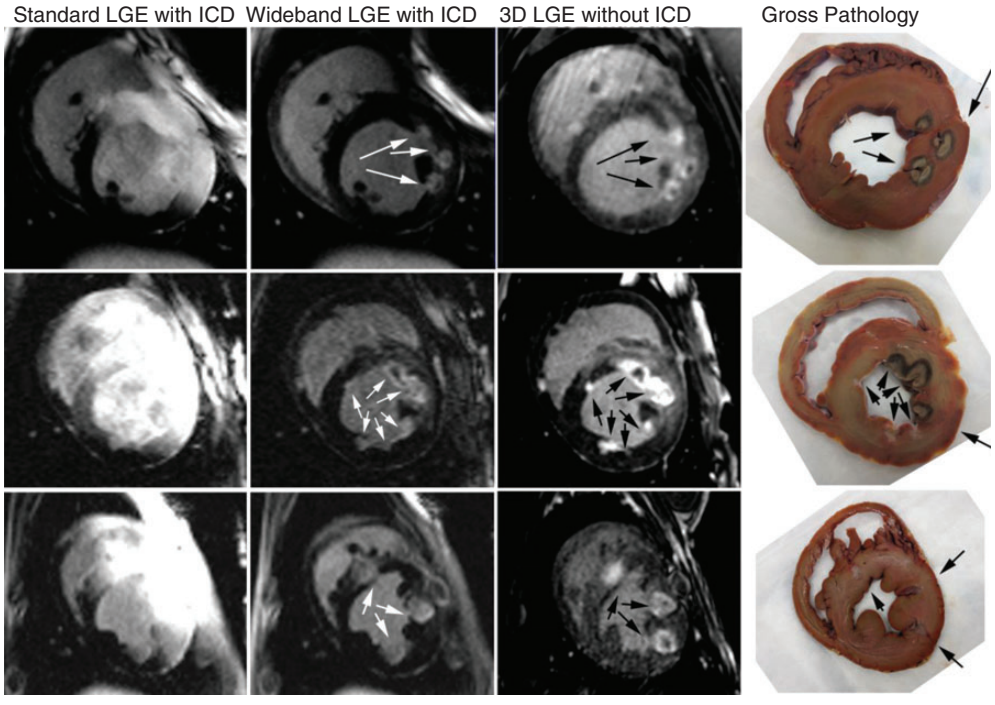


**Figure 2** Late gadolinium enhanced images of three different dogs with RF lesions acquired with standard (first column) and wideband (second column) LGE MRI with ICD. Unlike standard LGE MRI which exhibited image artefacts (bright regions) induced by ICD, wideband LGE MRI did not exhibit significant image artefacts and enabled complete visualization of RF lesions. Moreover, wideband LGE images with ICD correlated better with reformatted 3D LGE without ICD (third column) and gross pathology (fourth column) than standard LGE images with ICD. Each standard and wideband LGE image pair is displayed with identical grayscales.

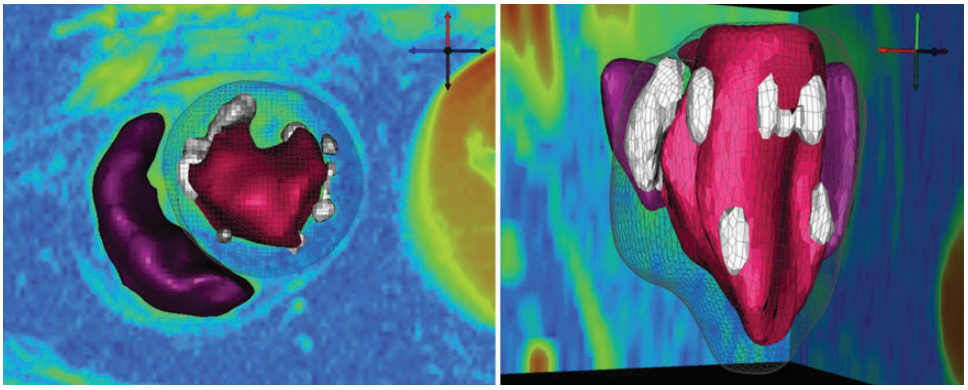

**Figure 3** Three-dimensional scar map generated from a stack of short-axis LGE images acquired using wideband LGE (same animal shown in *Figure 2*, top row). A similar 3D scar map was not generated from a stack of images acquired with standard LGE due to considerable image artefacts. Left ventricular and RV endocardial contours are show in red and purple, respectively. Scar areas are shown in white. Left ventricular epicardial surface is shown as a mesh. Apical view (left) and left lateral view with the RV on the far side (right).

# Discussion

This study demonstrates the feasibility of wideband LGE MRI for imaging ventricular scar without image artefacts induced by ICD at 3T. In 37 sets of images with different RF lesions, the mean image quality score (1−5; nondiagnostic to excellent) was significantly ($P < 0.001$) higher for wideband ($3.7 \pm 0.8$) than standard LGE MRI ($2.1 \pm 0.7$), and the mean artefact level (1−5; minimal to non-diagnostic) was significantly ($P < 0.001$) lower for wideband ($2.1 \pm 0.8$) than standard LGE MRI ($4.0 \pm 0.6$). Wideband LGE with ICD agreed better with 3D LGE without ICD and gross pathology than standard LGE with ICD. In summary, wideband LGE MRI suppresses image artefacts induced by ICD and enables accurate detection of myocardial scars within the SAR limit at 3 T.

This study has several discussion points worth noting. Firstly, in addition to the image artefacts which appear as hyper-intense signals, cardiac devices can also cause severe image distortion, spatial shifts, and signal loss due to intravoxel dephasing, all of which may be a problem when registering different MR images and quantifying scar volume. These effects can be minimized by using readout with a short echo time such as ultra-short TE pulse sequences. Secondly, this study did not include animals with ICD implantation (i.e. intracardiac leads). Our preliminary phantom experiment confirms that the frequency shift induced by leads is not enough to affect the efficacy of inversion pulses (*Figure 1*). Furthermore, our experience with LGE MRI (with a standard hyperbolic secant inversion pulse with frequency bandwidth $\sim 1$ kHz) in patients with cardiac devices at 1.5T and canines with pacemakers at 3 T (see Supplementary material online, *Figure S2*) suggests that the frequency shift induced by intracardiac leads is not enough to influence the efficacy of inversion pulses. Our experience is consistent with wideband LGE MRI results reported by Rashid *et al.*[13] A more thorough investigation is warranted to confirm our initial findings in patients with ICD. Thirdly, this study did not include any patients with ICD at 3 T due to safety concerns. A thorough study, like those reported at 1.5T,[11,12,18] is needed to verify the safety of performing MRI in patients with ICD at 3 T, which is beyond the scope of the current study. As described in the Methods section, the proposed wideband LGE MRI pulse sequence was designed specifically to deposit slightly lower global SAR than standard LGE MRI. Hence, our wideband LGE MRI is likely to pose no worse risk than standard LGE MRI at 3 T in patients with ICD. As new MR-compatible cardiac devices are developed, they are likely to activate new studies aimed to establish procedures for safe MRI of patients with ICD at 3 T. Fourthly, this study reports a limited histologic analysis of post-mortem myocardial tissue. A comprehensive histologic analysis of post-mortem myocardial tissues is warranted to fully evaluate the agreement between wideband LGE MRI and histology. We note, however, that it is not trivial to register a post-mortem tissue with its corresponding MR image acquired *in vivo*. Fifthly, this study did not report results of wideband LGE MRI at 1.5T. We performed a preliminary phantom experiment which showed that image artefact induced by ICD is similar between 1.5T and 3 T (see Supplementary material online, *Figure S3*). A more thorough investigation is warranted to understand the relationship between ICD electronics and off-resonance at different field strengths.

Late gadolinium enhanced MRI has been used to accurately identify myocardial scar.[19] The application of LGE MRI for identification of myocardial scars in patients with ICD has been limited due to image artefacts induced by cardiac devices.[9] This limitation was highlighted by a recent study using LGE MRI to identify ventricular scar to model VT circuits.[20] Because of this limitation, this prior study did not include patients with image artefacts from ICDs, which excluded the vast majority of patients with ICDs.[20] Given the growing number of patients with prophylactic ICD, it is clinically important to develop wideband LGE MRI and to widen its availability to all clinical MR scanners, including 3 T.

# Conclusion

In summary, this study demonstrates the feasibility of wideband LGE MRI for complete visualization of myocardial scars in the presence of ICD at 3T. Further studies in VT patients with a variety of cardiac

aetiologies encountered in clinical practice are warranted to evaluate the clinical utility of wideband LGE MRI.

# Supplementary material

Supplementary material is available at *Europace* online.

## Acknowledgements

The authors thank Andrew Plaisier for assistance with reformatting 3D LGE images.

## Funding

This work was supported in part by funding from the National Institutes of Health (K23HL115084, R01HL116895-01A1), American Heart Association (14GRNT18350028) and Ben B. and Iris M. Margolis Foundation. The content is solely the responsibility of the authors and does not necessarily represent the official views of the National Institutes of Health.

**Conflict of interest:** R.R. has been a consultant to Biosense Webster and has received speakers honorarium from Biotronik.

## References

1. Aliot EM, Stevenson WG, Almendral-Garrote JM, Bogun F, Calkins CH, Delacretaz E *et al.* EHRA/HRS Expert Consensus on Catheter Ablation of Ventricular Arrhythmias: developed in a partnership with the European Heart Rhythm Association (EHRA), a Registered Branch of the European Society of Cardiology (ESC), and the Heart Rhythm Society (HRS); in collaboration with the American College of Cardiology (ACC) and the American Heart Association (AHA). *Europace* 2009;**11**:771–817.
2. Stevenson WG, Khan H, Sager P, Saxon LA, Middlekauff HR, Natterson PD *et al.* Identification of reentry circuit sites during catheter mapping and radiofrequency ablation of ventricular tachycardia late after myocardial infarction. *Circulation* 1993;**88**:1647–70.
3. Ashikaga H, Sasano T, Dong J, Zviman MM, Evers R, Hopenfeld B *et al.* Magnetic resonance-based anatomical analysis of scar-related ventricular tachycardia: implications for catheter ablation. *Circ Res* 2007;**101**:939–47.
4. Mountantonakis SE, Park RE, Frankel DS, Hutchinson MD, Dixit S, Cooper J *et al.* Relationship between voltage map "channels" and the location of critical isthmus sites in patients with post-infarction cardiomyopathy and ventricular tachycardia. *J Am Coll Cardiol* 2013;**61**:2088–95.
5. Ranjan R. Magnetic resonance imaging in clinical cardiac electrophysiology. *Crit Rev Biomed Eng* 2012;**40**:409–26.
6. Reddy VY, Reynolds MR, Neuzil P, Richardson AW, Taborsky M, Jongnarangsin K *et al.* Prophylactic catheter ablation for the prevention of defibrillator therapy. *N Engl J Med* 2007;**357**:2657–65.
7. Marchlinski FE, Callans DJ, Gottlieb CD, Zado E. Linear ablation lesions for control of unmappable ventricular tachycardia in patients with ischemic and nonischemic cardiomyopathy. *Circulation* 2000;**101**:1288–96.
8. Kim RJ, Fieno DS, Parrish TB, Harris K, Chen EL, Simonetti O *et al.* Relationship of MRI delayed contrast enhancement to irreversible injury, infarct age, and contractile function. *Circulation* 1999;**100**:1992–2002.
9. Dickfeld T, Tian J, Ahmad G, Jimenez A, Turgeman A, Kuk R *et al.* MRI-Guided ventricular tachycardia ablation: integration of late gadolinium-enhanced 3D scar in patients with implantable cardioverter-defibrillators. *Circ Arrhythm Electrophysiol* 2011;**4**:172–84.
10. Tian J, Ahmad G, Mesubi O, Jeudy J, Dickfeld T. Three-dimensional delayed-enhanced cardiac MRI reconstructions to guide ventricular tachycardia ablations and assess ablation lesions. *Circ Arrhythmia Electrophysiol* 2012;**5**:e31–35.
11. Nazarian S, Halperin HR. How to perform magnetic resonance imaging on patients with implantable cardiac arrhythmia devices. *Heart Rhythm* 2009;**6**:138–43.
12. Sommer T, Naehle CP, Yang A, Zeijlemaker V, Hackenbroch M, Schmiedel A *et al.* Strategy for safe performance of extrathoracic magnetic resonance imaging at 1.5 tesla in the presence of cardiac pacemakers in non-pacemaker-dependent patients: a prospective study with 115 examinations. *Circulation* 2006;**114**:1285–92.
13. Rashid S, Rapacchi S, Vaseghi M, Tung R, Shivkumar K, Finn JP *et al.* Improved late gadolinium enhancement MR imaging for patients with implanted cardiac devices. *Radiology* 2014;**270**:269–74.
14. Fernandez-Armenta J, Berruezo A, Andreu D, Camara O, Silva E, Serra L *et al.* Three-dimensional architecture of scar and conducting channels based on high resolution ce-CMR: insights for ventricular tachycardia ablation. *Circ Arrhythmia Electrophysiol* 2013;**6**:528–37.
15. Griswold MA, Jakob PM, Heidemann RM, Nittka M, Jellus V, Wang J *et al.* Generalized autocalibrating partially parallel acquisitions (GRAPPA). *Magn Reson Med* 2002;**47**:1202–10.
16. Gupta A, Lee VS, Chung YC, Babb JS, Simonetti OP. Myocardial infarction: optimization of inversion times at delayed contrast-enhanced MR imaging. *Radiology* 2004;**233**:921–6.
17. McGann CJ, Kholmovski EG, Oakes RS, Blauer JJ, Daccarett M, Segerson N *et al.* New magnetic resonance imaging-based method for defining the extent of left atrial wall injury after the ablation of atrial fibrillation. *J Am Coll Cardiol* 2008;**52**:1263–71.
18. Nazarian S, Hansford R, Roguin A, Goldsher D, Zviman MM, Lardo AC *et al.* A prospective evaluation of a protocol for magnetic resonance imaging of patients with implanted cardiac devices. *Ann Intern Med* 2011;**155**:415–24.
19. Kim RJ, Chen EL, Lima JA, Judd RM. Myocardial Gd-DTPA kinetics determine MRI contrast enhancement and reflect the extent and severity of myocardial injury after acute reperfused infarction. *Circulation* 1996;**94**:3318–26.
20. Ashikaga H, Arevalo H, Vadakkumpadan F, Blake RC 3rd, Bayer JD, Nazarian S *et al.* Feasibility of image-based simulation to estimate ablation target in human ventricular arrhythmia. *Heart Rhythm* 2013;**10**:1109–16.